

69935
Breccia
127.6 grams



Figure 1: Photo of top exposed surface (T1) of 69935 showing abundant distribution of micrometeorite craters on polymict substrate. NASA S72-44455. Cube is 1 cm.

Introduction

69935 was chipped from the top of a 0.5 meter boulder at station 9, Apollo 16 – see picture in 69955. The top surface is covered with micrometeorite pits (figure 1), and this rock has been used to understand the flux of micrometeorites and erosion of boulder surface over the past 2 m.y. However, the exposure age obtained for the top of this boulder is not consistent with that of the sample from the bottom (69955), nor the data from track studies. No fillet has developed around the

boulder so it is thought to have been recently set out on top of the regolith (Sutton 1981).

Petrography

69935 is an apparently a polymict breccia that is texturally inhomogeneous (Ryder and Norman 1980). It contains a rather large white clast (figure 1, 2, 3). The matrix of 69935 appears to be that of a soil breccia (figures 4 and 5). However, the mineralogy of this



Figure 2: Photo of fresh-broken side (B1) of 69935. NASA S72-44459. Edge of cube is 1 cm.

sample has generally not been documented by petrologists.

Significant Clast

Anorthosite Clast:

A large white “clast” of anorthosite (1 x 2 cm) is exposed on the top, bottom and east end (E1) of the sample (figure 3). It has apparently not been studied.

Mineralogy

Metal: The only “mineral” that has been studied in 69935 is the Fe-Ni-Co metal grains. Taylor et al. (1976) performed annealing experiments on these grains to show that they can be significantly modified by heating – as in an ejecta blanket.

Chemistry

The chemical composition of the matrix of 69935 is rather similar to Apollo 16 soil (either the boulder was made of soil, or the soil was made from the boulder). There is a high abundance of meteoritical siderophile elements (Ir, Au etc). The REE data in Laul and Schmitt (1973) are inconsistent with their plot, indicating a misprint.

Radiogenic age dating

none

Cosmogenic isotopes and exposure ages

Behrmann et al. (1973) and Drozd et al. (1974) reported cosmic ray exposure ages of ^{81}Kr = 1.99 and ^{21}Ne = 1.4 m.y. - which is interpreted to be the age of South Ray Crater. Rancitelli et al. (1973) determined the cosmic

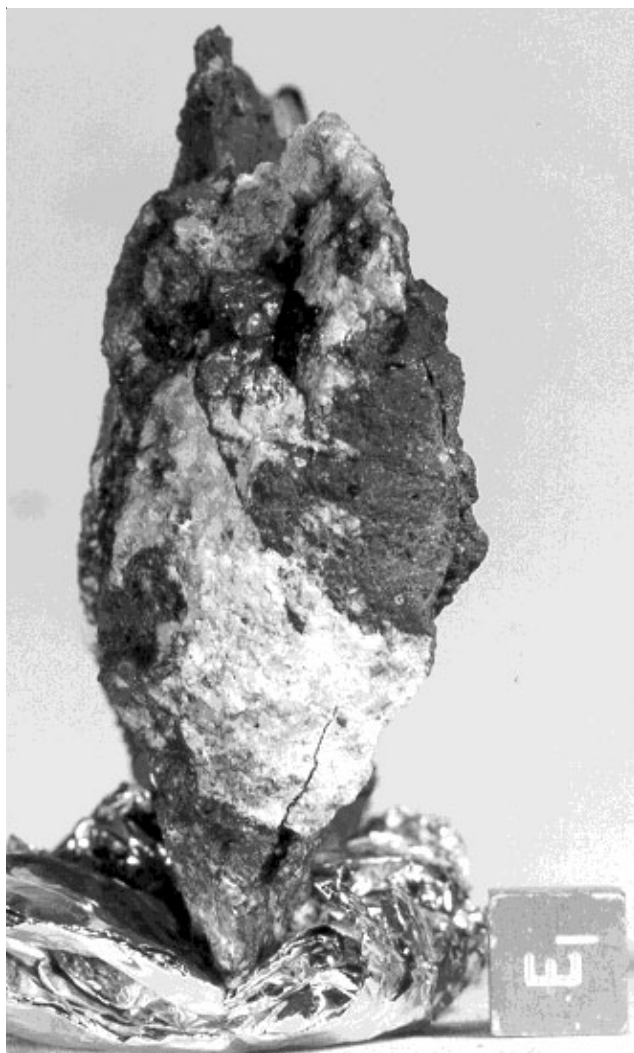


Figure 3: Side view of 69935 showing outcrop of large white (anorthosite?) clast. NASA S72-44457.

ray induced activity of $^{22}\text{Na} = 50 \text{ dpm/kg.}$, $^{26}\text{Al} = 159 \text{ dpm/kg.}$ and Fruchter et al. (1981) $^{53}\text{Mn} = 135 \text{ dpm/kg.}$ for 69935. Bhandari (1975) determined the activity of $^{26}\text{Al} = 300 \pm 140 \text{ dpm/kg.}$ for a surface sample.

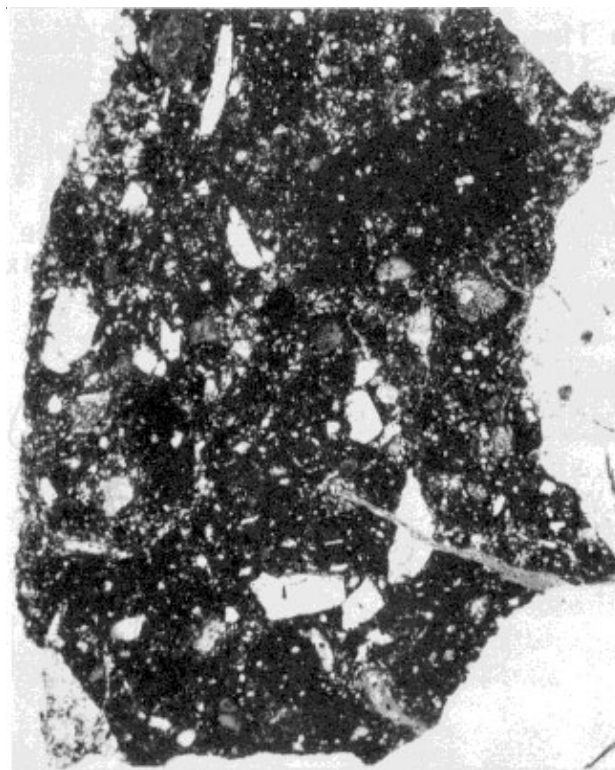


Figure 4: Thin section of glassy portion of 69935 (Ryder and Norman 1980). Width of field 1 cm.

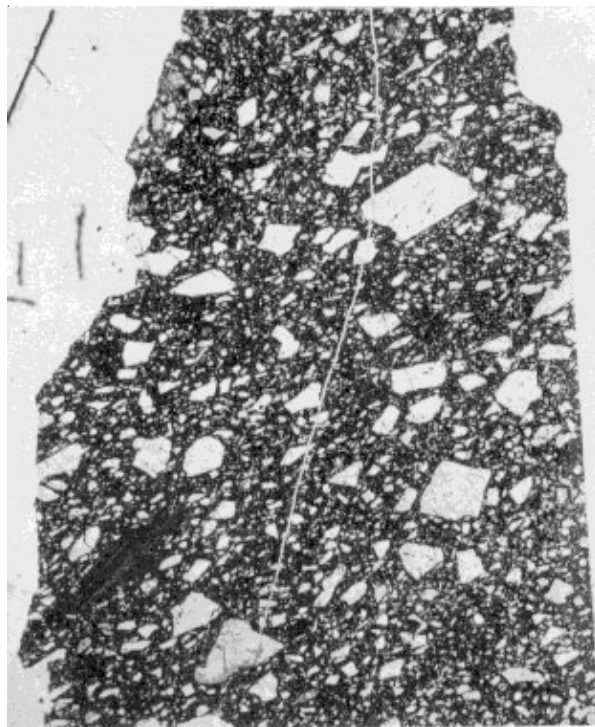


Figure 5: Thin section of matrix of 69935 (Ryder and Norman 1980). Width of field 1 cm.

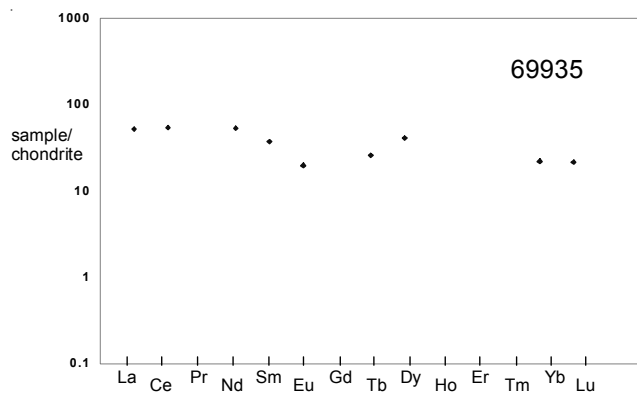


Figure 6: Normalized rare-earth-element diagram for 69935 (data from Laul and Schmitt 1973). However, this plot of their data doesn't correspond with their plot (figure 1 Laul and Schmitt).

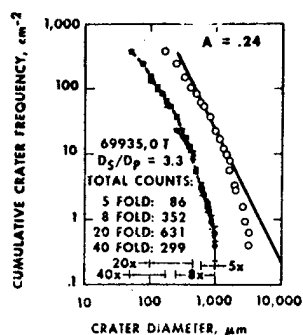


Figure 7: Size distribution of zap pits on 69935 (Neukum et al. 1973).

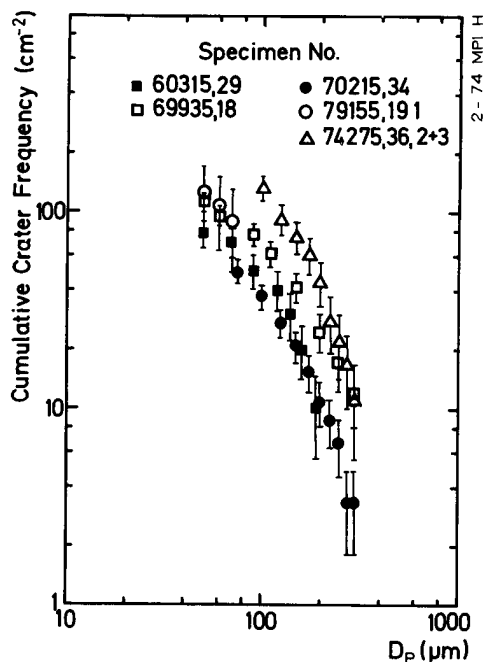


Figure 8: Size distribution of micrometeorite craters on several lunar samples including 69935 (Fechtig et al. 1974).

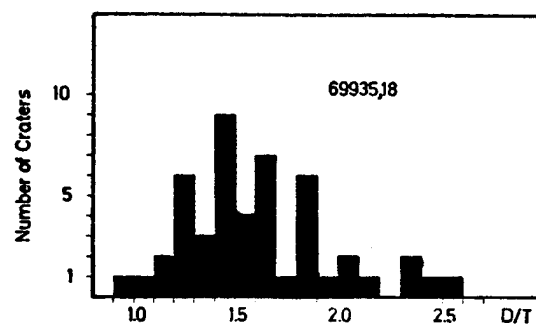


Figure 9: Histogram of diameter (D) vs. depth (T) ratio (D/T) of micrometeorite craters on surface of 69935 (Nagel et al. 1975).

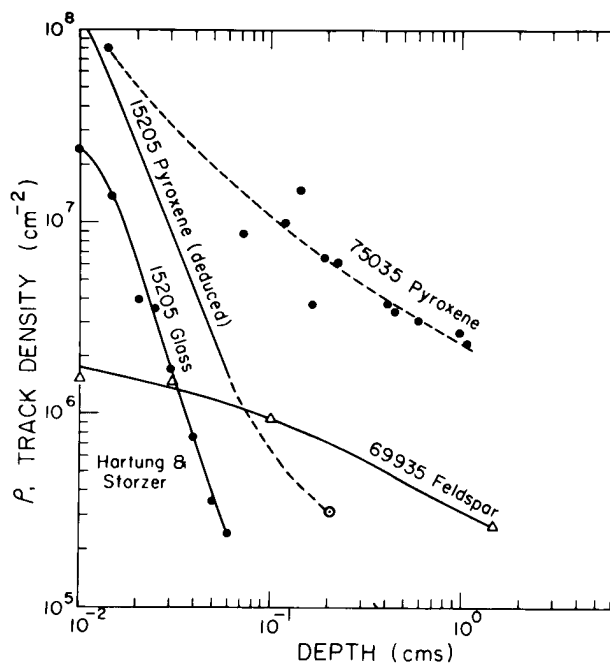


Figure 10: High energy track density as function of depth in "feldspar" in 69935 compared with track density in other rocks (Bhandari et al. 1977).

Other Studies

69935 was used for the study of micrometeorite pits (Morrison et al. 1973, Neukum et al. 1973, Fechtig et al. 1974 (figures 7 and 8). Nagel et al. (1975) studied the ratio of the diameter to depth of microcraters on the surface of 69935 and compared them with other samples (figure 9). Bhandari (1977) determined a cosmic ray track density/depth profile of feldspar (figure 10) and calculated an exposure age of only ~ 0.5 m.y. (significantly less than Drozd et al. 1974) – explained by local variation in spallation of surface material.

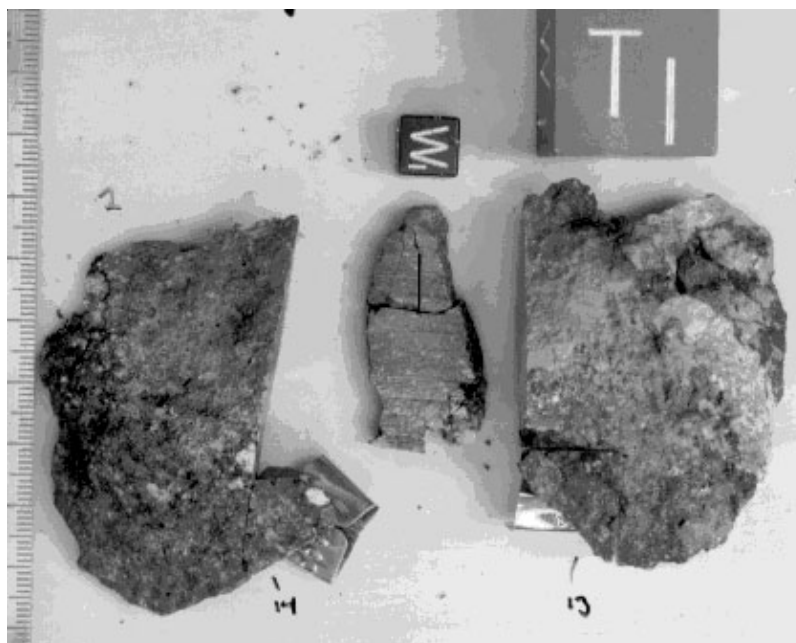
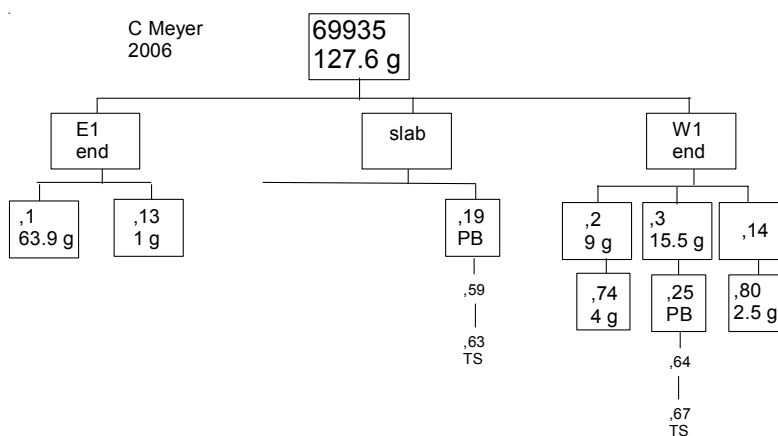


Figure 11: Photo illustrating cm and inch-sized orientation cubes along with slab cut from center of 69935. Compare with figure 1.



Processing

A lab was cut through the middle of 69935 (figure 11) perpendicular to the lunar surface to obtain a depth profile. The slab only cut thru the matrix of the boulder and did not sample the large white clast (which remains unstudied).

Table 1. Chemical composition of 69935.

<i>reference weight</i>	Ganapathy74	Laul 73	Rose 1973	Rancitelli 1973
SiO2 %			44.69	(b)
TiO2		0.35	(a) 0.22	(b)
Al2O3		29.5	(a) 31.47	(b)
FeO		4	(a) 2.34	(b)
MnO		0.045	(a) 0.03	(b)
MgO		4	(a) 2.63	(b)
CaO		17.2	(a) 17.97	(b)
Na2O		0.41	(a) 0.43	(b)
K2O		0.07	(a) 0.08	(b) 0.096 (d)
P2O5			0.15	(b)
S %				
<i>sum</i>				
Sc ppm		6	(a) 5.1	(b)
V		15	(a) 16	(b)
Cr		472	(a)	
Co		22	(a) 15	(b)
Ni	583	(c) 340	(a) 302	(b)
Cu			3.6	(b)
Zn	0.88	(c)		
Ga			1.8	(b)
Ge ppb	325	(c)		
As				
Se	190	(c)		
Rb	5.9	(c)	2	(b)
Sr				
Y			42	(b)
Zr		130	(a) 130	(b)
Nb				
Mo				
Ru				
Rh				
Pd ppb				
Ag ppb	1.3	(c)		
Cd ppb	6.6	(c)		
In ppb				
Sn ppb				
Sb ppb	3.63	(c)		
Te ppb	2.8	(c)		
Cs ppm	0.26	(c)		
Ba		110	(a) 115	(b)
La		12.3	(a) 10	(b)
Ce		33	(a)	
Pr				
Nd		24	(a)	
Sm		5.5	(a)	
Eu		1.11	(a)	
Gd				
Tb		0.94	(a)	
Dy		10	(a)	
Ho				
Er				
Tm				
Yb		3.6	(a) 2.9	(b)
Lu		0.52	(a)	
Hf		3.8	(a)	
Ta		0.45	(a)	
W ppb				
Re ppb	1.55	(c)		
Os ppb				
Ir ppb	12.7	(c) 8	(a)	
Pt ppb				
Au ppb	11.9	(c) 8	(a)	
Th ppm		2	(a)	2.52 (d)
U ppm	0.87	(c) 0.61	(a)	0.65 (d)
<i>technique: (a) INAA, (b) microchemical, (c) RNAA, (d) radiation counting</i>				